Cardiovasc Intervent Radiol (2019) 42:712–719
https://doi.org/10.1007/s00270-019-02163-3

CLINICAL INVESTIGATION NON-VASCULAR INTERVENTIONS

Virtual Guidance of Percutaneous Transthoracic Needle Biopsy with C-Arm Cone-Beam CT: Diagnostic Accuracy, Risk Factors and Effective Radiation Dose

Davide Fior[1] · Francesco Vacirca[1] · Davide Leni[1] · Fabio Pagni[2,3] · Davide Ippolito[1] · Luca Riva[1,2] · Sandro Sironi[2,4] · Rocco Corso[1]

Received: 20 August 2018 / Accepted: 4 January 2019 / Published online: 16 January 2019

Abstract

Purpose C-arm cone-beam computed tomography-guided transthoracic lung core needle biopsy (CBCT-CNB) is a safe and accurate procedure for the evaluation of patients with pulmonary nodules. The purpose of our study was to evaluate the diagnostic performance, complication rates and effective radiation dose of CBCT-CNB with virtual guidance.

Materials and Methods We retrospectively collected data regarding 375 CBCT-CNBs performed with virtual guidance (XperGuide—Philips Healthcare, Best, The Netherlands) from January 2010 to June 2015 on 355 patients (mean age, 68.1 years ± 11.8; age range, 31–88 years). Patients were divided into groups and compared based on the diagnostic failure and lesion size (15 mm cutoff). Diagnostic performance, complication rate and effective radiation dose were investigated. Variables influencing diagnostic performance and complications were assessed using Student's T test and Pearson's χ^2 test.

Results The sensitivity, specificity, positive and negative predictive value and accuracy for patients subjected to CNBs were 96.8%, 100%, 100%, 100% and 97.2%, respectively. Considering risk factors for pneumothorax, no significant differences were found regarding patient and lesion characteristics. Perilesional hemorrhage occurred more frequently in older patients ($p = 0.046$) and in smaller lesions ($p = 0.001$). Hemoptysis was significantly more frequent in patients with perilesional hemorrhage ($p = 0.01$). Mean effective radiation dose in CBCT-CNB was 7.12 ± 8.78 mSv.

Conclusions CBCT-CNB combined with virtual guidance is a reliable and accurate technique that allows exact localization of pulmonary lesions, effective preprocedural planning and real-time fluoroscopy altogether.

Introduction

When a suspicious pulmonary lesion is detected by any imaging modality, tissue samples are usually requested as part of the clinical assessment.

Bronchoscopy is often the first step, as it allows both direct observations of the lung lesion to evaluate its characteristics and extent and also to conduct tissue sampling. Although diagnostic rates of up to 80% have been reported depending on the method used to acquire tissues, bronchoscopic biopsy is limited to centrally located tumors that are visible from within the airways [1].

For lesions that cannot be approached through bronchoscopy, a transthoracic needle biopsy (TNB) is usually performed under image guidance.

✉ Davide Fior
davidefior85@gmail.com

1 Department of Diagnostic and Interventional Radiology, "San Gerardo" Hospital, Via Pergolesi 33, 20900 Monza, MB, Italy

2 School of Medicine, University of Milano-Bicocca, Via Cadore 48, 20900 Monza, MB, Italy

3 Department of Pathology, "San Gerardo" Hospital, Via Pergolesi 33, 20900 Monza, MB, Italy

4 Department of Diagnostic Radiology, ASST Papa Giovanni XXIII, Piazza OMS 1, 24127 Bergamo, BG, Italy

TNB is a minimally invasive diagnostic procedure for lung lesions suspicious of malignancy that enables the collection of a large amount of tissue, in order to obtain an exhaustive histopathological diagnosis along with therapy-related biomolecular tests [2–4].

Although TNB can be performed with fluoroscopic or ultrasonographic guidance depending on the characteristics and position of the pulmonary lesions, computed tomography (CT)-guided TNB has been widely performed in the diagnosis of small pulmonary lesions [5].

CT-guided TNB has been considered both accurate and safe. Geraghty et al. [6] reported an overall accuracy of CT-guided TNB of 93.5%; however, conventional CT guidance has limitations in the lack of real-time monitoring and gantry tilting for a more accessible needle pathway to the target lesion [7, 8].

The recent development of new angio-CT system software (Volume one shot—Toshiba) with rapid MPR reconstructions (8 s) partially overcomes these limitations allowing to obtain nearly real-time CT fluoroscopy-assisted oblique puncture images but still lacks the possibility to integrate real-time 2D fluoroscopy and 3D CT images [9].

For this reason, state-of-the-art C-arm cone-beam CT (CBCT) system has been introduced: This technique consists in a flat-panel volume CT in which a cone-beam X-ray tube and a flat-panel detector are integrated with a C-arm gantry, enabling both CT and fluoroscopy guidance.

This technique provides real-time guidance of the biopsy needle in addition to the advantages of CT guidance, decreasing the procedure time and number of needle passes compared with CT-guided procedures.

Furthermore, with the introduction of a new CBCT virtual navigation system (XperGuide—Philips Healthcare, Best, The Netherlands), it is now possible to create a virtual needle pathway upon the needle approach to the target nodule and to navigate the needle into the target after the operator determines the skin entry site and destination target based on preprocedural CBCT data. This guiding system has the technical strength of providing real-time fluoroscopic virtual navigation of biopsy needles based on volume CT data, allowing a flexible selection of the needle route under convenient operating conditions (Fig. 1).

Core biopsy needles are designed to collect a specimen intended for histopathological analysis rather than cytologic evaluation. Obtaining a core biopsy specimen increases the rate of a definite benign diagnosis from 52 to 91% [8, 10–13]. Although performing core biopsy improves the diagnostic yield of diagnosis, there is a slightly higher rate of complications such as pneumothorax and pulmonary hemorrhage [13–16].

Until now, there is only one article to our knowledge that evaluated the diagnostic outcomes and risk factors related to the use of this type of virtual guidance in a large population [17]: In this paper, the authors evaluated a large but heterogeneous study population that included patients that underwent CBCT-CNB with different types of virtual guidance and without virtual guidance.

Thus, the purpose of this study was to retrospectively evaluate the diagnostic performance, complication rates and effective radiation dose of C-arm cone-beam CT-guided core needle biopsy in a large monocentric European XperCT-guided lung CNB series.

Materials and Methods

Study Population

We collected data regarding 375 consecutive CNBs with virtual guidance (XperCT software with Allura Xper FD20 C-arm X-ray system; Philips Healthcare, Best, The Netherlands) performed from January 2010 to April 2015 on 355 patients (mean age, 68.1 years ± 11.8; age range, 31–88 years); 66.7% of the patients (236 out of 354) were men. All the procedures were performed by three interventional radiologists (F.V., D.L., R.C.,) with, respectively, 8-, 10- and 18-year experience in image-guided biopsies.

Before any procedure, patients signed the informed consent form relating to the procedure and to the use of anonymized data for study, in accordance with our institution's guidelines; ethical approval was obtained in compliance with our institutional review board.

Image Acquisition

The feasibility of the biopsy was evaluated reviewing the chest CT or PET-CT performed before the procedure, and each patient was positioned prone or supine depending on the location of the lesion and on the most appropriate access.

All CNBs were performed with a CBCT virtual navigation guidance system (XperCT and XperGuide software, Philips Healthcare, Best, The Netherlands) using 18-gauge semiautomatic biopsy needles (Biopsybell SRL, Mirandola, Modena, Italy) with a 17-gauge coaxial needle.

The needle path was planned on the first 180°–270° CBCT acquisition with the C-arm in order to define the shortest and safest trajectory, which could be checked on multiplanar reconstructions. In fluoroscopy, "bull's eye" approach was used to guide the entry point, and perpendicular approach to monitor the needle progression. CBCT and fluoroscopy images were merged real time to provide guidance on hybrid images. Further CBCT acquisition was performed to check needle placement and post-procedural complications.

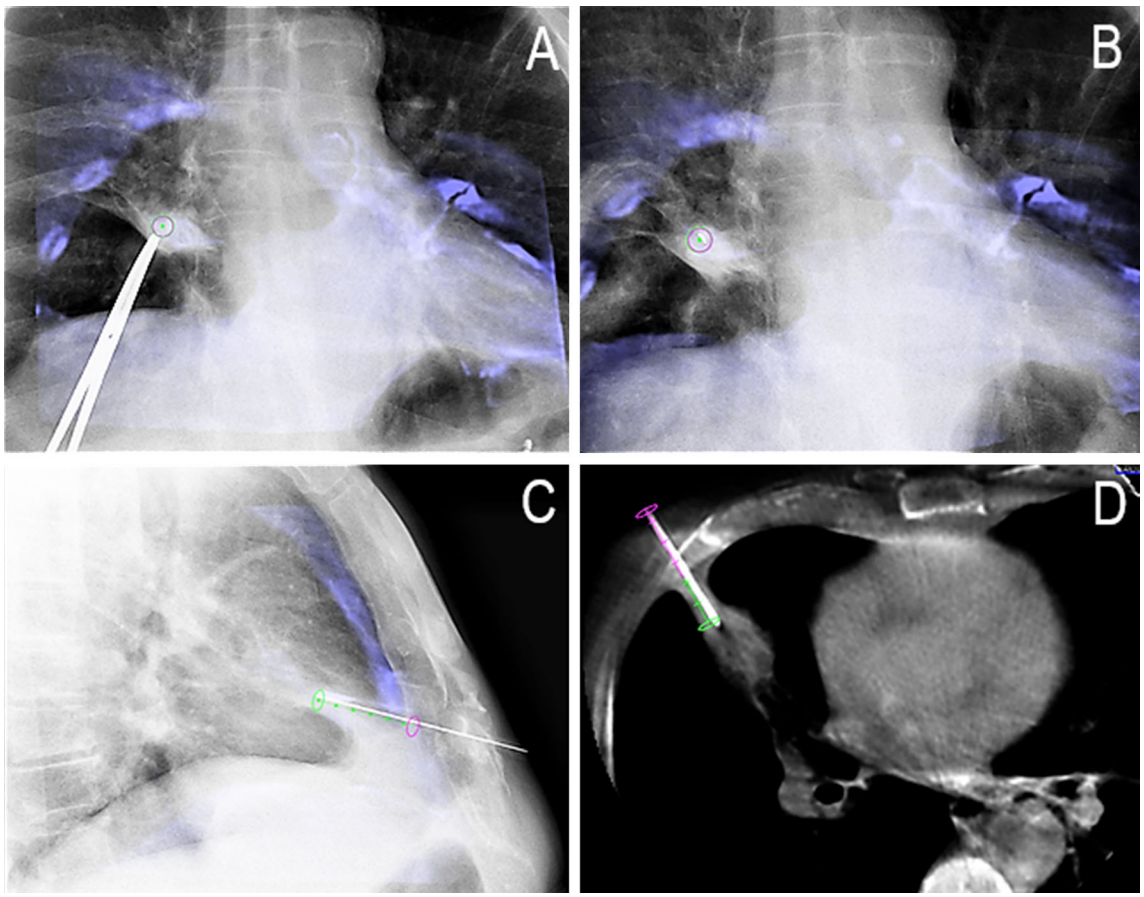

Fig. 1 **A**, **B** Real-time fluoroscopy with virtual guidance overlay in needle track perpendicular projection; **C** real-time fluoroscopy with virtual guidance overlay in needle track tangent projection; **D** cone-beam CT reconstruction with virtual guidance overlay and correct needle position

Biopsy Technique

Based on the predefined best skin-to-target biopsy path, XperGuide software automatically rotates the C-arm to the proper needle insertion position: The entrance point and the target point are directly superimposed over each other, showing the proper path of the needle (Fig. 1).

After the body surface puncture site is identified, disinfection and draping are performed with the puncture site at the center. Subsequently, the puncture site is anesthetized layer by layer using 2% lidocaine.

While the patient holds his breath, a 17-gauge guiding needle is advanced along the planned path under real-time fluoroscopy, with the hub of the needle projected over the tip along the superimposed virtual needle track.

After advancing for nearly half the distance to the target, the progression view is selected and the C-arm automatically swings to a 90 degrees projection tangent to the entry position; the needle tip is then advanced until it reaches the target at the end of the virtual needle color line.

Another CBCT is then performed to check the exact needle location within the target. If the needle tip is located correctly within the target lesion, then the stylet is removed and replaced coaxially by a 18-gauge semiautomatic biopsy needle, and approximately 1–2 cm of sample tissue is taken. The tissue specimen strip is fixed in 10% formalin, and multiple slides are prepared for histological analysis.

Eventually, the needle is removed and manual compression is applied at the puncture site for 30 s.

Post-biopsy complications are then investigated with post-procedural CBCT.

Data Collection

Analyzed clinical variables included patient demographics (patient age and sex), patient position (prone or supine), number and site of lesions, lesion size (defined as the maximum diameter on lung window setting images), number and size of biopsies, sample adequacy, procedure time and post-procedural complication such as pneumothorax, haemoptysis or perilesional hemorrhage.

Accuracy, sensitivity, specificity, positive predictive value (PPV) and negative predictive value (NPV) were determined by comparing the results of the biopsy with the

definitive histological diagnosis in cases of surgical resection. In all cases where nonsurgical therapy was performed, the result of the biopsy was compared with the clinical–radiological follow-up of the patient, with a minimum follow-up of 24 months.

CNB sensitivity was defined as the percentage of true positive (correctly identified malignant lesions) among all the actual positive patients (true positive + false negative); specificity is the percentage of true negative (correctly identified benign entities) among all the actual negative patients (true negative + false positives).

Patients were divided into groups and compared based on the diagnostic failure and lesion size (15 mm cutoff). Diagnostic failure was considered for biopsies that provided suboptimal quality or quantity of tissue, for which a definitive diagnosis and biological characterization of the lesion could not be established.

The effective dose (expressed in mSv) was estimated from dose–area product (expressed in mGy cm^2), using the previously described conversion factor for the Allura Xper FD20 system (0.31 mSv $Gycm^2$) that was obtained from a recent published phantom study [18]. All data were recorded in a dedicated database using Excel (Microsoft, Seattle, USA).

Statistical Analysis

Statistical differences regarding diagnostic success and post-procedural complications were evaluated with Student's t test for the following variables: age, lesion and size, number and size of cores.

Pearson's χ^2 test was used in the evaluation of the following variables: gender, lesion site, patient position, number of nodules, presence of procedure complications.

All statistical analyses were performed by using statistical software (SPSS, version 18.0; SPSS, Chicago, Illinois) using a 95% confidence interval.

Data are expressed as mean ± standard deviation for continuous variables.

Results

Lesion size ranged from 7 to 190 mm (mean size 38.5 ± 25.1 mm); 210 out of 375 (56%) were localized in the upper lobes (119 in the right lung and 91 in the left lung) and 212 (56.5%) were solitary lesions.

Histological results of the core needle biopsy procedures are summarized in Table 1. Sensitivity and specificity were 87.5% (CI 95% 0.820–0.893) and 100% (CI 95% 0.987–1.000). Positive predictive value (PPV), negative predictive value (NPV) and overall accuracy were 100%, 100% and 87.7%. Sensitivity was significantly lower for small lesions (57.1%, $p < 0.01$ for lesions ≤ 10 mm); in lesions with diameter above 20 mm, our diagnostic performance reached 90% in terms of sensitivity. It must be highlighted that on 36 out of 46 patients with a biopsy report of diagnostic failure, a repeat biopsy was performed; thus, while single procedure sensitivity is relatively low, patient sensitivity increases to 96.8% (305 correctly diagnosed patients out of 315 with malignant disease) and overall accuracy to 97.2%.

The mean effective dose through CBCT-CNBs was 7.12 ± 8.78 mSv.

Risk Factors for Diagnostic Failure (Table 2)

Diagnostic failure occurred more frequently in lesions smaller than 1.5 cm (< 1.5 cm vs > 1.5 cm; $p = 0.022$); also the number of samples and sample sizes differ significantly between the diagnostic success and diagnostic failure groups ($p = 0.044$ and $p = 0.028$, respectively). Furthermore, considering the complications, a significant higher incidence of perilesional hemorrhage was found in the diagnostic failure group in comparison with diagnostic success group ($p = 0.045$).

Risk Factors for CNB-Related Complications

Pneumothorax, perilesional hemorrhage and hemoptysis, respectively, occurred in 57 (15.2%), 41 (10.9%) and 9 (2.4%) procedures among 375 CNBs. We did not experience any case of air embolism or mortality in our study. Of the 57 pneumothoraxes, only 4 (6.6%) required drainage catheter insertion, whereas hemoptysis was managed with accurate patient observation until resolution or, if needed, with an operative bronchoscopy ($n = 3$) and administration of antifibrinolytics ($n = 6$). Self-limiting subcutaneous emphysema occurred in two cases. Mild thoracic pain was often recorded.

Considering risk factors for pneumothorax (Table 3), no significant differences were found regarding patient and lesion characteristics; a strong correlation between pneumothorax and hemoptysis was found ($p = 0.001$).

Perilesional hemorrhage (Table 4) occurred more frequently in older patients ($p = 0.046$) and in smaller lesions ($p = 0.001$). Furthermore, hemoptysis was more frequent in patients with perilesional hemorrhage, with a statistically significant p value ($p = 0.01$).

Discussion

In the last years, TNB has confirmed its central role in the percutaneous transthoracic evaluation of lung nodules; despite its theoretical and dreaded invasiveness, the current

Table 1 Histological results of 375 core needle biopsy procedures

L1. Non-diagnostic (n = 46; 12.2%)	Fibrosis/scattered acute and chronic inflammatory infiltrate (tumor capsule) n = 18
	Normal parenchyma samples n = 18
	Necrosis n = 10
L2. Benign (n = 46; 12.2%)	Acute pulmonary injury/interstitial pneumonia n = 25
	Reactive/reparative fibrotic nodules n = 15
	Nodular fibrosing pleuritis n = 3
	Wegener's granulomatosis n = 1
	Sarcoidosis n = 1
	Hamartoma n = 1
L3. Malignant, NOS (n = 9; 2.5%)	Malignant non-epithelial, NOS n = 4
	Lymphoproliferative, NOS n = 3
	Non-small cell lung cancer, NOS n = 2
L4. Diagnostic for specific malignant histotype (n = 274; 73.1%)	Lung adenocarcinomas n = 157
	Lung squamous cell carcinomas n = 51
	Lung large cell carcinoma n = 12
	Lung carcinoids n = 10
	Lung small cell carcinomas n = 9
	Mesotheliomas n = 5
	Rare histotypes and metastases n = 30

NOS not otherwise specified

Suboptimal quality of the sample that prevents further specification beyond a generic diagnosis of "malignant" NOS (small biopsy, excessive fragmentation, necrosis, paucity of neoplastic foci)

Optimal quality but insufficient quantity of the sample that prevents further specification beyond a generic diagnosis of "malignant" NOS (after application of immunohistochemistry panel, no specific tumor type is expressed)

Optimal quality but insufficient quantity of the sample that prevents further specification beyond a generic diagnosis of "non small cell lung carcinoma" (after application of immunohistochemistry panel)

technological support of the procedure is free from a significant rate of complications and shows good diagnostic performance [2].

The current paper reports a large series of CNBs performed with the CBCT virtual guidance in order to evaluate the diagnostic value and complication rates of lung CNB.

This procedure is conventionally performed under CT- or CT fluoroscopy guidance; however, these imaging techniques are often associated with limitations of in-plane imaging, real-time feedback, gantry sizes, etc.

CBCT is a technology in which CT images are acquired using a C-arm angiography system that rotates around the patient; this guidance technique has been applied to a broad range of interventional settings, including neurological, musculoskeletal and abdominal procedures [19–21]. With regard to the detection of pulmonary lesions, Higashihara et al. [22] showed that CBCT is as reliable as CT as imaging guidance technique in percutaneous interventional procedures because they demonstrated, in a phantom model, that CT and CBCT have a similar sensitivity in detecting parenchymal nodules.

Furthermore, the CBCT system can provide operators with more free space, it can enable effective control of patient breathing with real-time fluoroscopy during the procedure compared with the CT fluoroscopy system, and it can enable operators to avoid dangerous organs or overlying ribs that block the needle pathway to target lesions.

CBCT-guided lung CNB showed, in the majority of studies conducted on this technique, a specificity of 100% and a sensitivity over 95% [17, 18, 23, 24]. Our series reached 100% in specificity, PPV and NPV while sensitivity and overall accuracy settled at 87.5% and 87.7%, respectively; however, it has to be noted that, when considering patients and not procedures, sensitivity and accuracy noticeably increased (96.8% and 97.2%). This was due to the repeating of the biopsy, performed in a short period of time in order to avoid significant delays in the oncological management. The low procedure-related

Table 2 Univariate analysis for risk factors for diagnostic failure

Variable	Diagnostic failure (n = 46)	Diagnostic success (n = 329)	p value
Age (years)†	66.65 ± 11.22	68.31 ± 11.56	0.374*
Sex			
Male	28	221	0.397§
Female	18	108	
Patient position			0.632§
Supine	21	148	
Prone	25	181	
Lesion size			0.022§
≤ 15	8	24	
> 15	38	305	
Lesion location			0.107§
Upper and middle lobe	24	212	
Lower lobe	22	117	
No of tissue samplings	1.91	2.21	0.044*
Sample size (mm)	13.29	11.03	0.028*
Hemoptysis			0.304§
No	44	322	
Yes	2	7	
Pneumothorax			0.659§
No	38	280	
Yes	8	49	
Hemorrhage			0.045*
No	37	297	
Yes	9	32	

Unless otherwise indicated, data are numbers of patients

*p value was calculated with the independent sample t test

§p value was calculated with the Pearson χ^2 test

†Data are expressed as mean ± standard deviation

sensitivity could be related to the strictness of histopathological inclusion criteria for biopsies containing only foci of suspect cells that were, if necrotic or poorly preserved, labeled as unsatisfactory.

As for risk factors for diagnostic failure, lesion size (≤ 1.5 cm vs > 1.5 cm) was an independent risk factor; these results are in line with the findings obtained by other authors [17, 23].

Number of samples and sample sizes were a cause for the report resulting as unsatisfactory (p = 0.04 between mean core size in diagnostic success and diagnostic failure groups).

Furthermore, we found an higher incidence (p = 0.045) of perilesional hemorrhage in the diagnostic failure group in comparison with diagnostic success patients: A possible explanation is that a biopsied normal lung parenchyma with alveolar cavities could be more prone than pathological tissue to develop alveolar hemorrhage, being the natural compression and hemostasis weaker than in solid lesions.

The pneumothorax rate in our series was 15.2% and a strong correlation between pneumothorax and hemoptysis was found (p = 0.001); four cases (6.6%) required drainage catheter insertion.

These rates are similar to the previously reported ranges for pneumothorax rate (range 12.0–44.6%) and incidence of chest drainage catheter placement (range 0–32.7%) after CT-guided or CT fluoroscopy-guided biopsy [25–28].

The hemoptysis rate of 2.4% (9 of 375) is similar to the reported incidence (range 2.0–3.9%) of hemoptysis in CT-guided biopsy [27, 28].

Perilesional hemorrhage was found more often in older patients (p = 0.046) and in smaller lesions (p = 0.001; ≤ 1.5 cm vs > 1.5 cm). The higher rates of bleeding in smaller lesions may be due to the increased technical difficulty requiring more needle corrections; furthermore, when the biopsy is performed healthy lung parenchyma could be transfixed, contributing to the bleeding; moreover, the onset of hemoptysis was found more often (p = 0.01) in patients with perilesional hemorrhage.

Table 3 Univariate analysis of risk factors for pneumothorax

Variable	No (n = 318)	Yes (n = 57)	p value
Age (years)†	67.93 ± 12.13	69.07 ± 10.07	0.505*
Sex			
Male	213	36	0.574§
Female	105	21	24
Patient position			0.752§
Supine	147	22	
Prone	171	35	
Lesion size			0.106§
≤ 15	24	8	
> 15	294	49	
Lesion location			0.04§
Upper and middle lobe	206	30	
Lower lobe	112	27	
No of tissue samplings	1.91	2.21	0.191*
Sample size (mm)	13.04	13.01	0.46*
Hemoptysis	316	50	0.001#
No	316	50	
Yes	2	7	
Hemorrhage			0.415§
No	285	49	
Yes	33	8	

Unless otherwise indicated, data are numbers of patients

*p value was calculated with the independent sample t test

§p value was calculated with the Pearson χ^2 test

#p value was calculated with the Fischer's exact test

†Data are expressed as mean ± standard deviation

Table 4 Univariate analysis of risk factors for hemorrhage

Variable	No (n = 334)	Yes (n = 41)	p value
Age (years)†	67.34 ± 12.11	70.89 ± 9.19	0.046*
Sex			
Male	224	25	0.43§
Female	110	16	
Patient position			0.548§
Supine	193	24	
Prone	189	17	
Lesion size			
≤ 15	20	12	0.001§
> 15	314	29	
Lesion location			
Upper and middle lobe	209	27	0.68§
Lower lobe	125	14	
No of tissue samplings†	2.14 ± 0.89	2.16 ± 0.94	0.078*
Sample size (mm)†	13.11 ± 5.80	12.27 ± 5.35	0.379*
Hemoptysis			0.01#
No	329	37	
Yes	5	4	
Pneumothorax			0.4§
No	285	33	
Yes	49	8	

Unless otherwise indicated, data are numbers of patients

*p value was calculated with the independent sample t test

§p value was calculated with the Pearson χ^2 test

#p value was calculated with the Fischer's exact test

†Data are expressed as mean ± standard deviation

Lee et al. [17] performed a similar evaluation of risk factors in a large group of CBCT-guided biopsies using one of two different virtual guidance techniques (iGuide-Siemens Medical Solutions or XperGuide–Philips Healthcare) or without virtual guidance.

Comparing to our study, we obtained similar results regarding the overall accuracy of the procedures; furthermore, Lee et al. found that the use of virtual guidance was a significant protective factor for pneumothorax and hemoptysis. A possible explanation is that the use of virtual guidance could reduce unnecessary redirections, but further studies for validation of these findings are warranted.

In our study, the mean estimated effective dose through CBCT-guided biopsies was 7.12 ± 8.78 mSv; unfortunately, the dose estimates reported in different studies of CT-guided CNB are scarcely comparable because of biopsy procedure variables that may impact on radiation exposure and because of methodological differences in estimating the effective dose [29, 30]; therefore, further investigations of radiation exposure comparing the CBCT and the conventional CT procedures are needed.

Our study has some limitations: firstly, our evaluation was based on a monocentric retrospective analysis; secondly, our study design did not include a comparison between the diagnostic accuracy of CBCT and that of CT-guided biopsies.

In conclusion, our results demonstrate that CBCT biopsy combined with XperCT virtual guidance is a reliable and accurate technique, which allows exact localization of pulmonary lesions, effective preprocedural planning and real-time fluoroscopy altogether; this technique provides a valuable alternative to CT guidance, while at the same time freeing up CT systems for diagnostic examinations.

Compliance with Ethical Standards

Conflict of interest The authors declare that they have no conflict of interest.

Ethical Approval All procedures performed in studies involving human participants were in accordance with the ethical standards of

the institutional and/or national research committee and with the 1964 Helsinki Declaration and its later amendments or comparable ethical standards.

Informed Consent Informed consent was obtained from all individual participants included in the study.

References

1. Herth FJF, Eberhardt R, Ernst A. The future of bronchoscopy in diagnosing, staging and treatment of lung cancer. Respiration. 2016;73:399–409.
2. Gould MK, Donington J, Lynch WR, et al. Evaluation of individuals with pulmonary nodules: When is it lung cancer? Diagnosis and management of lung cancer, 3rd ed: American College of Chest Physicians evidence-based clinical practice guidelines. Chest. 2013;143:e93S–120S.
3. Winer-Muram HT. The solitary pulmonary nodule. Radiology. 2006;239(1):34–49.
4. Heck SL, Blom P. Berstad A accuracy and complications in computed tomography fluoroscopy guided needle biopsies of lung masses. Eur Radiol. 2006;16(6):1387–92.
5. Hiraki T, Mimura H, Gobara H, et al. CT floroscopy-guided biopsy of 1,000 pulmonary lesions performed with 20-gauge coaxial cutting needles: diagnostic yield and risk factors for diagnostic failure. Chest. 2009;136(6):1612–7.
6. Geraghty PR, Kee ST, McFarlane G, Razavi MK, Sze DY, Dake MD. CT-guided transthoracic needle aspiration biopsy of pulmonary nodules: needle size and pneumothorax rate. Radiology. 2003;229(2):475–81.
7. Carlson SK, Felmlee JP, Bender CE, et al. CT floroscopy-guided biopsy of the lung or upper abdomen with a breath-hold monitoring and feedback system: a prospective randomized controlled clinical trial. Radiology. 2005;237(2):701–8.
8. Yankelevitz DF, Vazquez M, Henschke CI. Special techniques in transthoracic needle biopsy of pulmonary nodules. Radiol Clin N Am. 2000;38(2):267–79.
9. Sato R, Aramaki T, Yoza K, et al. "Direct MPR": a useful tool for oblique CT fluoroscopy-assisted puncture. Cardiovasc Intervent Radiol. 2017;40(8):1261–6.
10. Arakawa H, Nakajima Y, Kurihara Y, Niimi H, Ishikawa T. CT-guided transthoracic needle biopsy: a comparison between automated biopsy gun and fine needle aspiration. Clin Radiol. 1996;51(7):503–6.
11. Boiselle PM, Shepard JA, Mark EJ, et al. Routine addition of an automated biopsy device to fine-needle aspiration of the lung: a prospective assessment. AJR Am J Roentgenol. 1997;169(3):661–6.
12. Haramati LB. CT-guided automated needle biopsy of the chest. AJR Am J Roentgenol. 1995;165(1):53–5.
13. Klein JS, Salomon G, Stewart EA. Transthoracic needle biopsy with a coaxially placed 20-gauge automated cutting needle: results in 122 patients. Radiology. 1996;198(3):715–20.
14. Goralnik CH, O'Connell DM, el Yousef SJ, Haaga JR. CT-guided cutting-needle biopsies of selected chest lesions. AJR Am J Roentgenol. 1988;151(5):903–7.
15. Beslic S, Zukic F, Milisic S. Percutaneous transthoracic CT guided biopsies of lung lesions; fine needle aspiration biopsy versus core biopsy. Radiol Oncol. 2012;46(1):19–22.
16. Yeow K-M, Tsay P-K, Cheung Y-C, Lui K-W, Pan K-T, Chou AS-B. Factors affecting diagnostic accuracy of CT-guided coaxial cutting needle lung biopsy: retrospective analysis of 631 procedures. J Vasc Interv Radiol. 2003;14(5):581–8.
17. Lee SM, Park CM, Lee KH, Bahn YE, Kim JI, Goo JM. C-arm cone-beam CT-guided percutaneous transthoracic needle biopsy of lung nodules: clinical experience in 1108 patients. Radiology. 2014;271(1):291–300.
18. Strocchi S, Colli V, Conte L, et al. Multidector CT fluoroscopy and cone-beam CT-guided percutaneous transthoracic biopsy: comparison based on patient doses. Radiat Prot Dosim. 2012;151:162–5.
19. Hirota S, Nakao N, Yamamoto S, et al. Cone-beam CT with flat-panel-detector digital angiography system: early experience in abdominal interventional procedures. Cardiovasc Intervent Radiol. 2006;29:1034–8.
20. Kang SE, Lee JW, Kim JH, et al. Percutaneous sacroplasty with the use of C-arm flat-panel detector CT: technical feasibility and clinical outcome. Skeletal Radiol. 2011;40:453–60.
21. Carrafiello G, Fontana F, Mangini M, et al. Initial experience with percutaneous biopsies of bone lesions using XperGuide cone-beam CT (CBCT): technical note. Radiol Med. 2012;117:1386–97.
22. Higashihara H, Osuga K, Azuma T, et al. Detection of pulmonary nodules by C-arm CT using a phantom lung: comparison with CT. Acta Radiol. 2011;52:964–8.
23. Floridi C, Muollo A, Fontana F, et al. C-arm cone-beam computed tomography needle path overlay for percutaneous biopsy of pulmonary nodules. Radiol Med. 2014;119(11):802–7.
24. Cheng YC, Tsai SH, Cheng, et al. Percutaneous transthoracic lung biopsy: comparison between C-arm cone-beam CT and conventional CT guidance. Transl Oncol. 2015;8(4):258–64.
25. Ohno Y, Hatabu H, Takenaka D, et al. CT-guided transthoracic needle aspiration biopsy of small (, or = 20 mm) solitary pulmonary nodules. AJR Am J Roentgenol. 2003;180(6):1665–9.
26. Hiraki T, Mimura H, Gobara H, et al. Incidence of and risk factors for pneumothorax and chest tube placement after CT floroscopy-guided percutaneous lung biopsy: retrospective analysis of the procedures conducted over a 9-year period. AJR Am J Roentgenol. 2010;194(3):809–14.
27. Yeow KM, Su IH, Pan KT, et al. Risk factors of pneumothorax and bleeding: multivariate analysis of 660 CT-guided coaxial cutting needle lung biopsies. Chest. 2004;126(3):748–54.
28. Kazerooni EA, Lim FT, Mikhail A, Martinez FJ. Risk of pneumothorax in CT-guided transthoracic needle aspiration biopsy of the lung. Radiology. 1996;198(2):371–5.
29. Choi JW, Park CM, Goo JM, et al. C-arm cone-beam CT-guided percutaneous transthoracic needle biopsy of small ($\leq$ 20 mm) lung nodules: diagnostic accuracy and complications in 161 patients. Am J Roentgenol. 2012;199:322–30.
30. Kim GR, Hur J, Lee SM, et al. CT fluoroscopy-guided lung biopsy versus conventional CT-guided lung biopsy: a prospective controlled study to assess radiation doses and diagnostic performance. Eur Radiol. 2011;21:232–9.